

**Spin-1 Ising model: Exact damage-spreading relations and numerical simulations**A. S. Anjos,<sup>1,\*</sup> A. M. Mariz,<sup>1,†</sup> F. D. Nobre,<sup>2,‡</sup> and I. G. Araujo<sup>3,§</sup><sup>1</sup>*Departamento de Física Teórica e Experimental, Universidade Federal do Rio Grande do Norte, Campus Universitário, Caixa Postal 1641, 59072-970 Natal–Rio Grande do Norte, Brazil*<sup>2</sup>*Centro Brasileiro de Pesquisas Físicas, Rua Xavier Sigaud 150, 22290-180 Rio de Janeiro, RJ, Brazil*<sup>3</sup>*Departamento de Física, Universidade Federal de Roraima, BR 174 s/n, Campus de Paricarana, Jardim Floresta I, 69310-270 Boa Vista, RR, Brazil*

(Received 19 May 2008; published 3 September 2008)

The nearest-neighbor-interaction spin-1 Ising model is investigated within the damage-spreading approach. Exact relations involving quantities computable through damage-spreading simulations and thermodynamic properties are derived for such a model, defined in terms of a very general Hamiltonian that covers several spin-1 models of interest in the literature. Such relations presuppose translational invariance and hold for any ergodic dynamical procedure, leading to an efficient tool for obtaining thermodynamic properties. The implementation of the method is illustrated through damage-spreading simulations for the ferromagnetic spin-1 Ising model on a square lattice. The two-spin correlation function and the magnetization are obtained, with precise estimates of their associated critical exponents and of the critical temperature of the model, in spite of the small lattice sizes considered. These results are in good agreement with the universality hypothesis, with critical exponents in the same universality class of the spin-1/2 Ising model. The advantage of the present method is shown through a significant reduction of finite-size effects by comparing its results with those obtained from standard Monte Carlo simulations.

DOI: [10.1103/PhysRevE.78.031105](https://doi.org/10.1103/PhysRevE.78.031105)

PACS number(s): 05.50.+q, 05.10.Ln, 64.60.F–, 75.10.Hk

**I. INTRODUCTION**

Computer simulations [1] have become one of the most important tools in the study of physical systems nowadays. Essentially, this happened due to a fast advance in computer technology, in such a way that hard computational tasks—considered as essentially intractable some years ago—are becoming more and more investigated. Among many types of numerical simulations, the Monte Carlo (MC) method [2,3] appears as a commonly used technique, being applied successfully to a wide variety of systems. In a standard MC simulation one investigates the dynamical (i.e., out-of-equilibrium) behavior, or the long-time (presumably at equilibrium) properties of a given physical system, by following the time evolution of a single copy of it, with the dynamical variables being updated according to certain dynamical rules. The major limitation of this method concerns the constraint for simulating finite systems, and consequently, the undesired obstacle of dealing appropriately with the finite-size effects. Usually, one analyzes the largest possible sizes, taking into consideration the computing facilities available, and makes extrapolations to the infinite-size limit (i.e., thermodynamic limit).

A different type of MC simulation, known as the “damage-spreading” (DS) technique [4,5], turned out to be very effective for studying both the dynamical and static properties of statistical models. In these simulations, one investigates the time evolution of the Hamming distance between two (originally identical) copies of a given system,

with a perturbation (or damage) introduced in one of them at the initial time. In order to ensure that possible differences between the two copies, at later times, are only due to their initial damage, the two copies are set to evolve under the same updating rules and sequences of random numbers. In what concerns investigations of dynamic properties, the DS method has been applied to many magnetic systems, like the Ising [4–10] and Potts [11–14] models, among others. Intriguingly, the propagation of the initial damage depended on the particular dynamical procedure used for the simulations.

Usually one is also interested in obtaining equilibrium properties from numerical simulations; in what concerns the DS technique, this possibility is raised when exact relations involving quantities computable from DS simulations and thermodynamic properties were derived for the Ising ferromagnet [15]. This led to a new numerical procedure to estimate quantities like order parameters and two-spin correlation functions, and its implementation was done, as an illustrative example, through simulations for the ferromagnetic Ising model on a square lattice, resulting in a significant reduction of finite-size effects [15]. Further on, more general exact relations were derived for other systems, like the Potts [16], Ashkin-Teller [16], discrete  $N$ -vector [17], and  $(N_\alpha, N_\beta)$  [18] models. These relations are valid for any ergodic dynamical procedure applied to translationally invariant systems, leading, as expected, to thermodynamic properties that do not depend on the particular kind of dynamics employed.

Recently, the corresponding exact relations were applied in DS simulations of the  $q$ -state Potts [19] and Ashkin-Teller [20] ferromagnets on a square lattice. In what concerns the Potts model, the efficiency of the method was illustrated through precise estimates of the critical exponents  $\beta$  and  $\eta$ , associated, respectively, with the magnetization and two-spin correlation function, for  $q=2, 3$ , and 4. For the Ashkin-Teller model, the analysis of such quantities was restricted to the Baxter line, well known for its continuously varying critical

\*asafilho@dfte.ufrn.br

†anancias@dfte.ufrn.br

‡Corresponding author. fdnobre@cbpf.br

§ijanilio@hotmail.com

exponents [21]; the method provided accurate estimates, in spite of the small lattice sizes considered, yielding agreements of the computed critical exponents with the corresponding exact results within four decimal places. In this latter case, besides a significant reduction of finite-size effects with respect to standard MC simulations, the well-known universality breakdown along the Baxter line was detected, with the results suggesting smooth and continuous variations of the critical exponents, which represents a non-trivial task within MC simulations.

In the present work we investigate the nearest-neighbor-interaction spin-1 Ising model through the DS technique. It is important to recall that, according to the universality hypothesis, the critical exponents associated with a phase transition in a spin-1 Ising model, on a given lattice should coincide with those of the corresponding spin-1/2 Ising model on a lattice of the same dimension. Herein, besides deriving exact DS relations, we test the universality hypothesis for the spin-1 Ising model on a square lattice. In the next section we derive exact relations between quantities computable through DS simulations and thermodynamic properties for the spin-1 Ising model. These relations are valid for any ergodic dynamical procedure applied on a translationally invariant system. In Sec. III, we define the numerical procedure to be used in order to implement the DS simulations by making use of such exact relations and illustrate the method by applying it to the ferromagnetic nearest-neighbor-interaction spin-1 Ising model on a square lattice. Finally, in Sec. IV we present our conclusions.

## II. EXACT DAMAGE-SPREADING RELATIONS FOR THE SPIN-1 ISING MODEL

Let us consider the nearest-neighbor-interaction spin-1 Ising model defined in terms of the Hamiltonian

$$\mathcal{H} = -J \sum_{\langle ij \rangle} S_i S_j - L \sum_{\langle ij \rangle} S_i^2 S_j^2 - D \sum_i S_i^2 - H \sum_i S_i, \quad (2.1)$$

where  $S_i = \pm 1, 0$  and the summation  $\sum_{\langle ij \rangle}$  runs over all pairs of nearest-neighbor sites of a given regular lattice. Since in the derivation that follows one requires translational invariance with respect to the site magnetizations, the coupling constants  $J$  and  $L$  should be both positive; however, in what concerns the fields  $D$  and  $H$ , there are no restrictions on their signs. For the exceptional case  $J=H=0$ , one has to avoid situations where combinations of  $(L, D)$  may lead to a stable antiferromagnetic state at low temperatures.

In order to investigate DS properties, one should deal with two copies ( $A$  and  $B$ ) of the system, characterized by the variables  $\{S_i^A\}$  and  $\{S_i^B\}$ , respectively. We define a damaged site, at a given time  $t$ , when  $S_i^A(t) \neq S_i^B(t)$ ; there are six possible types of damaged sites in the present system. For computational purposes, it is more convenient to work with the following binary variables,

$$\Pi_i = \frac{1}{2} S_i (1 + S_i), \quad (2.2)$$

$$\Theta_i = 1 - S_i^2, \quad (2.3)$$

$$\Omega_i = \frac{1}{2} S_i (S_i - 1). \quad (2.4)$$

Below, we list all six possible types of damages associated to a given site  $i$ :

$$(1) \quad \Pi_i^A = 1 \quad \text{and} \quad \Pi_i^B = 0 \quad (S_i^A = 1, S_i^B \neq 1), \quad (2.5)$$

$$(2) \quad \Pi_i^A = 0 \quad \text{and} \quad \Pi_i^B = 1 \quad (S_i^A \neq 1, S_i^B = 1), \quad (2.6)$$

$$(3) \quad \Theta_i^A = 1 \quad \text{and} \quad \Theta_i^B = 0 \quad (S_i^A = 0, S_i^B \neq 0), \quad (2.7)$$

$$(4) \quad \Theta_i^A = 0 \quad \text{and} \quad \Theta_i^B = 1 \quad (S_i^A \neq 0, S_i^B = 0), \quad (2.8)$$

$$(5) \quad \Omega_i^A = 1 \quad \text{and} \quad \Omega_i^B = 0 \quad (S_i^A = -1, S_i^B \neq -1), \quad (2.9)$$

$$(6) \quad \Omega_i^A = 0 \quad \text{and} \quad \Omega_i^B = 1 \quad (S_i^A \neq -1, S_i^B = -1). \quad (2.10)$$

If one considers the two copies  $A$  and  $B$  in thermal equilibrium, the probabilities that the above-defined damages appear at site  $i$  are given, respectively, by

$$p_1 = \langle \Pi_i^A (1 - \Pi_i^B) \rangle_t, \quad (2.11)$$

$$p_2 = \langle (1 - \Pi_i^A) \Pi_i^B \rangle_t, \quad (2.12)$$

$$p_3 = \langle \Theta_i^A (1 - \Theta_i^B) \rangle_t, \quad (2.13)$$

$$p_4 = \langle (1 - \Theta_i^A) \Theta_i^B \rangle_t, \quad (2.14)$$

$$p_5 = \langle \Omega_i^A (1 - \Omega_i^B) \rangle_t, \quad (2.15)$$

$$p_6 = \langle (1 - \Omega_i^A) \Omega_i^B \rangle_t, \quad (2.16)$$

where  $\langle \dots \rangle_t$  represents time averages over trajectories in phase space. Let us now define differences between these probabilities,

$$E \equiv p_1 - p_2 = \langle \Pi_i^A \rangle_t - \langle \Pi_i^B \rangle_t, \quad (2.17)$$

$$F \equiv p_3 - p_4 = \langle \Theta_i^A \rangle_t - \langle \Theta_i^B \rangle_t, \quad (2.18)$$

$$G \equiv p_5 - p_6 = \langle \Omega_i^A \rangle_t - \langle \Omega_i^B \rangle_t. \quad (2.19)$$

Next, we will show that under some constraints to be imposed for the time evolution of copies  $A$  and  $B$ , the quantities  $E$ ,  $F$ , and  $G$  will be directly related to thermodynamic properties.

Let us then consider the initial time ( $t=0$ ) with the two copies in thermal equilibrium. Below, we define six different types of boundary conditions to be imposed on these time evolutions for  $t \geq 0$  [denoted herein by  $e_i$  ( $i=1, 2, \dots, 6$ )].

Time evolution  $e_1$ : In this case we consider a boundary condition for the variable  $S_i^B$  at the central site of the lattice,  $S_0^B \neq 1$  (i.e.,  $\Pi_0^B = 0$ ), for all times  $t \geq 0$ . This represents a ‘‘source of damage’’ at the central site; all remaining spins of

the lattice, on both copies, are let free to evolve following the corresponding dynamical procedure.

Time evolution  $e_2$ : The two copies should evolve freely according to a given dynamical procedure, except for their central sites, which are restricted to  $\Pi_0^A=1$  and  $\Pi_0^B=0$ , for all times  $t \geq 0$ .

Time evolution  $e_3$ : The central site of copy  $B$  is restricted to  $\Theta_0^B=0$  for all times  $t \geq 0$ . All remaining sites, on both copies  $A$  and  $B$ , are let free to evolve under a certain dynamical procedure.

Time evolution  $e_4$ : The two copies should evolve freely according to a given dynamical procedure, except for their central sites, which are restricted to  $\Theta_0^A=1$  and  $\Theta_0^B=0$ , for all times  $t \geq 0$ .

Time evolution  $e_5$ : Copy  $A$  evolves with no restrictions; the central site of copy  $B$  is restricted to  $\Omega_0^B=0$  for all times  $t \geq 0$ .

Time evolution  $e_6$ : The two copies should evolve freely, except for their central sites, which are restricted to  $\Omega_0^A=1$  and  $\Omega_0^B=0$ , for all times  $t \geq 0$ .

In order to obtain exact relations involving the quantities of Eqs. (2.17)–(2.19) and correlation functions, as well as order parameters, we will make use of the time evolutions defined above. Since different boundary conditions are associated with different time evolutions, they will lead, in the long-time limit, to distinct exact relations, as described below.

Considering the time evolution  $e_1$  and assuming that copies  $A$  and  $B$  evolve in time under an ergodic dynamics, one has that

$$\langle \Pi_i^A \rangle_t = \langle \Pi_i \rangle_T, \quad \langle \Pi_i^B \rangle_t = \frac{\langle (1 - \Pi_0) \Pi_i \rangle_T}{\langle 1 - \Pi_0 \rangle_T}, \quad (2.20)$$

where  $\langle \dots \rangle_T$  stands now for thermal averages with no constraints. In the equations above,  $\langle \Pi_i^A \rangle_t$  represents the probability for the variable  $S_i^A$  presenting the value  $+1$  with no restrictions, whereas  $\langle \Pi_i^B \rangle_t$  is the conditional probability for finding the variable  $S_i^B=1$ , provided that  $S_0^B \neq 1$ .

If our system is translationally invariant, then one may write

$$E(e_1) = \frac{\langle \Pi_0 \Pi_i \rangle_T - \langle \Pi_0 \rangle_T \langle \Pi_i \rangle_T}{1 - \langle \Pi_0 \rangle_T} = \frac{C_{0i}^{(11)} + C_{0i}^{(12)} + C_{0i}^{(21)} + C_{0i}^{(22)}}{2(2 - m - p)}, \quad (2.21)$$

where  $C_{0i}^{(\alpha\beta)}$  ( $\alpha, \beta=1, 2$ ) are correlation functions,

$$C_{0i}^{(\alpha\beta)} = \langle S_0^\alpha S_i^\beta \rangle_T - \langle S_0^\alpha \rangle_T \langle S_i^\beta \rangle_T, \quad (2.22)$$

whereas  $m$  and  $p$  are order parameters,

$$m = \langle S_0 \rangle_T, \quad p = \langle S_0^2 \rangle_T, \quad (2.23)$$

known as magnetization and polarization, respectively. Since we are supposing translational invariance, the quantities above represent standard thermodynamic quantities: namely, two-spin correlation functions ( $C_{0i}^{(\alpha\beta)}$ ), magnetization ( $m$ ), and polarization ( $p$ ) per site, respectively.

Now, considering the time evolution  $e_2$ , one gets

$$\langle \Pi_i^A \rangle_t = \frac{\langle \Pi_0 \Pi_i \rangle_T}{\langle \Pi_0 \rangle_T}, \quad \langle \Pi_i^B \rangle_t = \frac{\langle (1 - \Pi_0) \Pi_i \rangle_T}{\langle 1 - \Pi_0 \rangle_T}, \quad (2.24)$$

in such a way that

$$E(e_2) = \frac{\langle \Pi_0 \Pi_i \rangle_T - \langle \Pi_0 \rangle_T \langle \Pi_i \rangle_T}{\langle \Pi_0 \rangle_T (1 - \langle \Pi_0 \rangle_T)} = \frac{C_{0i}^{(11)} + C_{0i}^{(12)} + C_{0i}^{(21)} + C_{0i}^{(22)}}{(m + p)(2 - m - p)}. \quad (2.25)$$

Similar procedures for the time evolutions  $e_3, \dots, e_6$ , yield, respectively,

$$F(e_3) = \frac{\langle \Theta_0 \Theta_i \rangle_T - \langle \Theta_0 \rangle_T \langle \Theta_i \rangle_T}{1 - \langle \Theta_0 \rangle_T} = \frac{C_{0i}^{(22)}}{p}, \quad (2.26)$$

$$F(e_4) = \frac{\langle \Theta_0 \Theta_i \rangle_T - \langle \Theta_0 \rangle_T \langle \Theta_i \rangle_T}{\langle \Theta_0 \rangle_T (1 - \langle \Theta_0 \rangle_T)} = \frac{C_{0i}^{(22)}}{p(1 - p)}, \quad (2.27)$$

$$G(e_5) = \frac{\langle \Omega_0 \Omega_i \rangle_T - \langle \Omega_0 \rangle_T \langle \Omega_i \rangle_T}{1 - \langle \Omega_0 \rangle_T} = \frac{C_{0i}^{(11)} - C_{0i}^{(12)} - C_{0i}^{(21)} + C_{0i}^{(22)}}{2(2 + m - p)}, \quad (2.28)$$

$$G(e_6) = \frac{\langle \Omega_0 \Omega_i \rangle_T - \langle \Omega_0 \rangle_T \langle \Omega_i \rangle_T}{\langle \Omega_0 \rangle_T (1 - \langle \Omega_0 \rangle_T)} = \frac{C_{0i}^{(11)} - C_{0i}^{(12)} - C_{0i}^{(21)} + C_{0i}^{(22)}}{(p - m)(2 + m - p)}. \quad (2.29)$$

Therefore, the computational procedure may be implemented by performing the appropriate simulations, with the above-mentioned time evolutions; after that, one may use Eqs. (2.21) and (2.25)–(2.29) in order to obtain the order parameters and correlation functions of the model.

In what follows, we will obtain additional exact relations for the order parameters by considering copies  $A$  and  $B$  evolving in time in the presence of specific external magnetic fields without fixing any spin of these copies (this is to be denoted hereafter as time evolution  $e_7$ ). For that, at the initial time ( $t=0$ ), one should have both copies in thermal equilibrium and with their spins reversed, i.e.,  $S_i^A(t=0) = -S_i^B(t=0)$  on all sites [except, for the trivial cases,  $S_i^A(t=0) = S_i^B(t=0) = 0$ ]. Further on, both copies should evolve in time under opposite small magnetic fields,  $H^A = -H^B = H$  ( $\forall t \geq 0$ ). Now, considering the quantities  $E$  and  $G$ , defined in Eqs. (2.17) and (2.19), one gets, respectively,

$$\langle \Pi_i^A \rangle_t = \langle \Pi_i \rangle_T, \quad \langle \Pi_i^B \rangle_t = \langle 1 - \Pi_i \rangle_T, \quad (2.30)$$

$$\langle \Omega_i^A \rangle_t = \langle \Omega_i \rangle_T, \quad \langle \Omega_i^B \rangle_t = \langle 1 - \Omega_i \rangle_T, \quad (2.31)$$

which lead to

$$E(e_7) = \langle S_i^2 \rangle_T + \langle S_i \rangle_T - 1, \quad G(e_7) = \langle S_i^2 \rangle_T - \langle S_i \rangle_T - 1, \quad (2.32)$$

$$\langle S_i \rangle_T = \frac{1}{2}[E(e_7) - G(e_7)], \quad \langle S_i^2 \rangle_T = \frac{1}{2}[E(e_7) + G(e_7)] + 1. \quad (2.33)$$

Therefore, for the order parameters, in which case one may be interested in a wide range of temperatures (sometimes far

away from criticality), the single time evolution  $e_7$  is less time consuming from the computational point of view. In what concerns correlation functions, one should apply the above procedure, characterized by the time evolutions  $e_1, \dots, e_6$ ; although this requires larger computational times, one is usually restricted to a small range of temperatures (close to criticality).

It is important to recall that, in contrast to the results of Ref. [15], the exact relations above do not depend on the ‘‘Hamming distance’’ between two configurations and are written in terms of quantities that are independent of the particular dynamical rule; therefore, these relations hold for any ergodic dynamical procedure.

In the next section we describe the numerical procedure to be used in order to implement the DS simulations to an specific model, by making use of the exact relations derived above.

### III. IMPLEMENTATION OF THE TECHNIQUE: THE FERROMAGNETIC SPIN-1 ISING MODEL ON THE SQUARE LATTICE

In this section we illustrate the method by applying it to the ferromagnetic nearest-neighbor-interaction spin-1 Ising model on a square lattice, i.e.,  $L=D=0$  in Eq. (2.1). For the simulations of the time evolutions  $e_1, \dots, e_6$ , we will consider  $H=0$ , whereas in the single time evolution  $e_7$ , small magnetic fields will be applied to copies  $A$  and  $B$ .

First of all, let us describe how we compute the dependence of the correlation functions on the distance between spins. For the two-site correlation functions one should take into account the central site of the lattice and an arbitrary site  $i$ , a distance  $r$  apart. It should be mentioned that, in most of the cases, on a square lattice, there are four sites  $i$  with the same distance  $r$  from the central site. However, there are a few exceptions, where one may have more than four sites with the same distance  $r$  from the central site: if one considers a unit lattice spacing, one has 8 sites whose distance to the central site is  $\sqrt{5}$  and 12 sites for which this distance is 5. Therefore, it is always possible to define the correlation functions as the average values,

$$C^{(\alpha\beta)}(r) = \frac{1}{4} \sum_{i(r)} C_{0i}^{(\alpha\beta)}, \quad (3.1)$$

where  $C_{0i}^{(\alpha\beta)}$  are defined in Eq. (2.22). In addition to that,  $\sum_{i(r)}$  corresponds to a summation over four sites with the same distance  $r$  from the central site; in the exceptional cases where there may be more than four sites with the same distance  $r$  from the central site, the extra sites are not taken into account in the averages of Eq. (3.1).

In the present model, the relevant quantities, computable through the DS technique described in the previous section, correspond to the critical temperature and critical exponents associated with the correlation function  $C^{(11)}(r)$  and the magnetization  $m$ . As usual, within DS simulations, we will follow the time evolution of copies  $A$  and  $B$  of the system, for a given temperature  $T$ , subjected to the same thermal noise and same set of random numbers. Initially, we let one copy

(e.g.,  $\{S_i^A\}$ ) evolve for  $t_{\text{eq}}$  MC steps towards equilibrium; as standard practice, our unit of time (1 MC step) consists in a complete sweep of the lattice. We assume that the equilibrium state is attained when one observes small fluctuations in time on thermodynamic quantities, like magnetization and energy. After the equilibration process of copy  $A$  (time  $t=0$ ), this configuration is stored (as a new copy  $A_0$ ), which will remain untouched; then, the time evolution  $e_1$  (characterized by its corresponding constraint, as described in the previous section) is carried for copies  $A$  and  $B$  in such a way that one obtains, after  $t_{\text{av}}$  MC steps,  $E(e_1)$ . Now, recovering configuration  $A_0$ , which will become configuration  $A$  for time evolution  $e_2$ , one performs such an evolution in order to get  $E(e_2)$ . The procedure is repeated for time evolutions  $e_3, \dots, e_6$  in such a way that one may compute the correlation functions and order parameters, making use of the exact relations derived in the previous section. In the time evolution  $e_7$  copy  $A$  is considered in the presence of a sufficiently small magnetic field and then taken to equilibrium; at this time ( $t=0$ ), copy  $B$  is defined with spins, as well as the magnetic field, reversed with respect to those of copy  $A$ .

One should recall that the exact relations of the previous section hold for any ergodic dynamics applied to translationally invariant systems. Herein, we have considered a simulation in which all sites of the lattice are visited in a sequential way, and each spin  $S_i^\mu(t)$  ( $\mu=A,B$ ), at time  $t$ , is updated according to the following rules.

(i) A possible new state  $S_i^\mu(t+1)$  is chosen at random, with  $S_i^\mu(t+1) \neq S_i^\mu(t)$ , from which one calculates the change in energy,  $\Delta\mathcal{H}^\mu = \mathcal{H}^\mu(t+1) - \mathcal{H}^\mu(t)$ .

(ii) Then, one can define the probability,

$$p_i^\mu(t) = \frac{1}{1 + \exp(\beta\Delta\mathcal{H}^\mu)} \quad [\beta = 1/(k_B T)]. \quad (3.2)$$

(iii) By introducing a random number  $z_i(t)$ , uniformly distributed in the interval  $[0, 1]$ , one performs the change if  $z_i(t) < p_i^\mu(t)$ ; otherwise, the spin  $S_i^\mu(t)$  is not updated.

It is important to mention that the spin-updating procedure is the same for all time evolutions  $e_1, \dots, e_7$ ; however, in the latest case (time evolution  $e_7$ ) the energy change for  $t \geq 0$ ,  $\Delta\mathcal{H}^\mu$ , should be computed by taking the Hamiltonian of Eq. (2.1) in the presence of the corresponding (i.e., opposite) external magnetic fields for copies  $A$  and  $B$ .

We investigated the model on square lattices of linear sizes  $L=50$  and  $100$ , with periodic boundary conditions. For the correlation functions, the distance  $r$  was measured with respect to the central site, located at coordinates  $(L/2, L/2)$ . We have always started copy  $A$  with all spins  $S_i^A=1$  ( $\forall i$ ); then, this copy was let to evolve towards equilibration for  $t_{\text{eq}}$  MC steps, after which, the second copy (copy  $B$ ) was created. In the case of time evolution  $e_7$ , we have attributed small positive numbers to the dimensionless quantity  $[H/(k_B T)]$ ; in order to find its appropriate value, this quantity was successively decreased in such a way to find no dependence of the particular choice of the magnetic fields on our results, taking into account the error bars. In the present simulations we have considered  $[H/(k_B T)]=0.0001$ . For the evolution towards equilibrium, we verified that  $t_{\text{eq}}=1 \times 10^4$



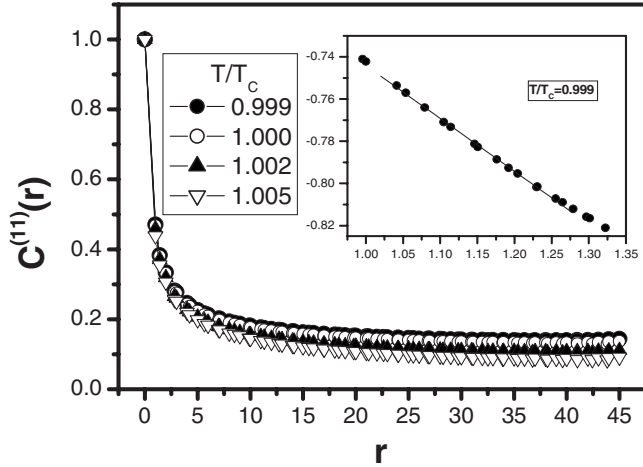


FIG. 1. The correlation function  $C^{(11)}(r)$  versus  $r$  (square lattice of linear size  $L=100$ ) for typical temperature ratios  $T/T_C$ , near criticality. The slowest decay was found for  $T/T_C=0.999$ , in which case the plot of  $\log_{10}[C^{(11)}(r)]$  versus  $\log_{10} r$  is presented in the inset, leading to the estimate  $\eta=0.2507 \pm 0.0025$ .

( $L=50$ ) and  $t_{\text{eq}}=5 \times 10^4$  ( $L=100$ ) MC steps were sufficient for a fulfillment of the equilibrium conditions described above, i.e., small fluctuations in the magnetization and energy. When using time evolutions  $e_1, \dots, e_6$ , the thermal averages were carried over times  $t_{\text{av}}=2.4 \times 10^5$  ( $L=50$ ) and  $t_{\text{av}}=2.4 \times 10^6$  ( $L=100$ ) MC steps, whereas in the calculation of the order parameters (time evolution  $e_7$ ) smaller times were necessary, i.e.,  $t_{\text{av}}=1.5 \times 10^4$  ( $L=50$ ) and  $t_{\text{av}}=3 \times 10^5$  ( $L=100$ ) MC steps. In order to reduce the possible effects of correlations in time, we only consider, in our time averages, data at each time interval of 3 MC steps. Therefore, each time average consists in an average over  $t_{\text{av}}/3$  measurements. It is important to stress that, due to large fluctuations, the times  $t_{\text{av}}$  considered herein are much larger than those used in simpler ferromagnetic models [15,19]. In addition to that, in order to improve the statistics, as well as to reduce possible dependence on sequences of random numbers, each simulation was repeated for  $M$  different samples. For the linear size  $L=50$  we considered  $M=50$  (time evolutions  $e_1, \dots, e_6$ ) and  $M=20$  (time evolution  $e_7$ ), whereas in the case  $L=100$  we used  $M=25$  (time evolutions  $e_1, \dots, e_6$ ) and  $M=20$  (time evolution  $e_7$ ).

It should be mentioned that although the critical temperature of the present model is not known exactly, there are accurate estimates for it; in terms of the variable  $u = \exp[-J/(k_B T)]$ , one has, e.g., from a transfer-matrix approach,  $u_C \approx 0.554066$  (Ref. [22]), and from an extensive low-temperature series expansion up to 79th order,  $u_C = 0.554065(5)$  (Ref. [23]). Based on these results, in the following analysis we will express our results in terms of the approximate critical-temperature estimate,

$$u_C = 0.554065 \Rightarrow \frac{k_B T_C}{J} = 1.693556 \dots \quad (3.3)$$

In Fig. 1 we present the correlation function  $C^{(11)}(r)$  versus  $r$  for a square lattice of linear size  $L=100$ . In this case,

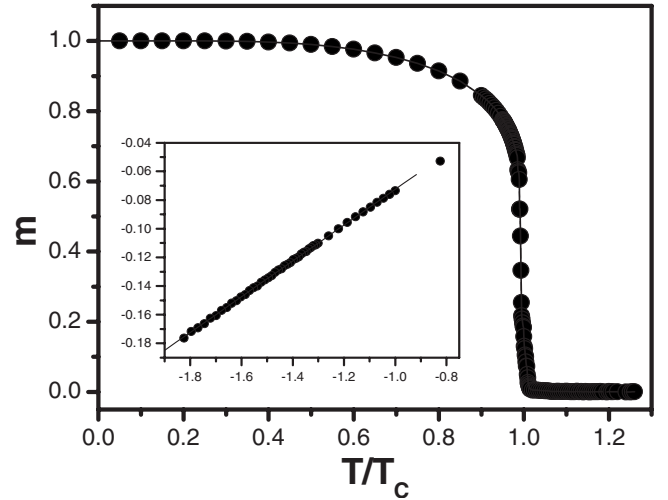


FIG. 2. The magnetization  $m$  versus  $T/T_C$  for a square lattice of linear size  $L=100$ . The inset shows the plot of  $\log_{10}(m)$  versus  $\log_{10}(1 - T/T_C)$ , leading to the estimate  $\beta=0.1249 \pm 0.0003$ .

our criterion for locating the critical temperature (associated with the finite size of the system considered) consists in searching for the temperature ratio  $T/T_C$  at which the function  $C^{(11)}(r)$  presents the slowest decay with  $r$ . For clarity, in Fig. 1 we present only the correlation functions associated with four typical different ratios  $T/T_C$ , including the one of slowest decay, although we have investigated other temperature ratios as well (in fact, we have swept temperatures around criticality by considering increments of 0.001 in  $T/T_C$ ). The power-law behavior

$$C^{(11)}(r) \sim r^{-\eta} \quad (r \rightarrow \infty) \quad (3.4)$$

is verified in the inset of Fig. 1 for the temperature ratio  $T/T_C=0.999$ , with the associated critical exponent  $\eta = 0.2507 \pm 0.0025$ . It is important to recall that, according to the universality hypothesis, the critical exponents of a given model should not depend on its microscopic details, but rather on global properties like the dimension of the lattice and the symmetry of the order parameter; therefore, the spin-1 and spin-1/2 Ising models on lattices of the same dimension should present the same set of critical exponents. The present estimate is in agreement with the well-known exact result for the spin-1/2 Ising model on a square lattice, i.e.,  $\eta=1/4$ . In spite of the small lattice size considered, the temperature associated with the slowest-decay correlation function presents a relative discrepancy of 0.001 with respect to the critical temperature of Eq. (3.3); this discrepancy is expected to decrease even further for larger lattice sizes. This tendency was confirmed through the computation of the correlation function  $C^{(11)}(r)$  for a square lattice of linear size  $L=50$ , as will be shown below.

In Fig. 2 we exhibit the magnetization  $m$  versus  $T/T_C$  for a square lattice of linear size  $L=100$ , obtained by using the time evolution  $e_7$ . The log-log plot in the inset yields the associated critical exponent  $\beta=0.1249 \pm 0.0003$ , with the critical temperature of Eq. (3.3); in this case, the critical temperature of Eq. (3.3) led to the best linear fit in such a

log-log plot. Again, the present critical-exponent estimate is in agreement with the universality hypothesis when compared with the well-known exact result for the spin-1/2 Ising model on a square lattice, i.e.,  $\beta=1/8$ . It is important to mention that similar results could also be achieved for the magnetization by using time evolutions  $e_1, \dots, e_6$ , although a larger computational effort would be required in obtaining the magnetization curve for such a large temperature range (cf. Ref. [19]). In spite of the reasonably small lattice size considered, one observes in Fig. 2 a magnetization curve that is essentially characterized by a lack of fluctuations—even near criticality—with weak finite-size effects; this represents one of the greatest advantages of the present DS simulations. In fact, the critical-exponent estimates for a square lattice of linear size  $L=100$  (from Figs. 1 and 2) coincide, within the error bars, with those obtained through the DS technique for the size  $L=50$ . These results suggest that the linear size  $L=100$  is sufficient, at least in what concerns the DS technique, for reliable critical-exponent estimates. Combining the results of the correlation function  $C^{(1)}(r)$  with those of the magnetization, one may calculate an average value for the critical temperature; such an average yields  $(k_B T_C / J) = 1.692\,709 \pm 0.000\,847$ , i.e.,  $u_C = 0.553\,901 \pm 0.000\,164$ , which agree with the results of Eq. (3.3), within the error bars.

We now illustrate the efficiency of the present method when compared with standard MC simulations. In Fig. 3 we verify the power-law behavior of Eq. (3.4) by presenting the plots of the correlation function  $C^{(1)}(r)$  versus  $r$ , in logarithmic scale, with the data obtained from a standard MC simulation and the present DS procedure. The data exhibited correspond, in each case, to the slowest decay of the correlation function  $C^{(1)}(r)$ , found from a sweep in  $T/T_C$  around the approximate value of Eq. (3.3) with increments of 0.001, as mentioned above, and using the same simulation parameters for each linear size  $L$  (e.g.,  $t_{\text{eq}}$  and  $t_{\text{av}}$ ). In Fig. 3(a) we compare the result of a standard MC simulation with those of the DS technique for a linear size  $L=50$ ; one notices a significant reduction of finite-size effects in the latter approach with respect to the first one, shown through the following features: (i) The ratio  $T/T_C$ , associated with the slowest decay of the correlation function  $C^{(1)}(r)$ , is closer to the approximate value of Eq. (3.3) in the DS technique [ $(T/T_C) = 0.995$ ] than in the MC method [ $(T/T_C) = 0.990$ ]. (ii) The linear fit, obtained in the log-log plot of the DS results, is more reliable in the sense that it covers a larger range of values of  $r$ . However, if one restricts the analysis, in each case, to those sets of points associated with the best linear fits, one gets essentially the same estimates (within the error bars) for the exponent  $\eta$  in both techniques, i.e.,  $\eta = 0.2429 \pm 0.0075$  (linear fit considering 7 points from the MC procedure) and  $\eta = 0.2505 \pm 0.0008$  (linear fit with 11 points from the DS method), which are both in agreement with the exact result for the spin-1/2 Ising model on a square lattice. For increasing values of  $r$ , the finite-size effects get pronounced, as usual, leading to points out of the linear regime; keeping in mind that the power-law behavior of Eq. (3.4) is expected to hold in the limit  $r \rightarrow \infty$ , one notices that the linear regime in Fig. 3(a) occurs typically for  $1 < r < 6$  ( $4 < r < 12$ ) in the MC (DS) approach. Therefore, for this

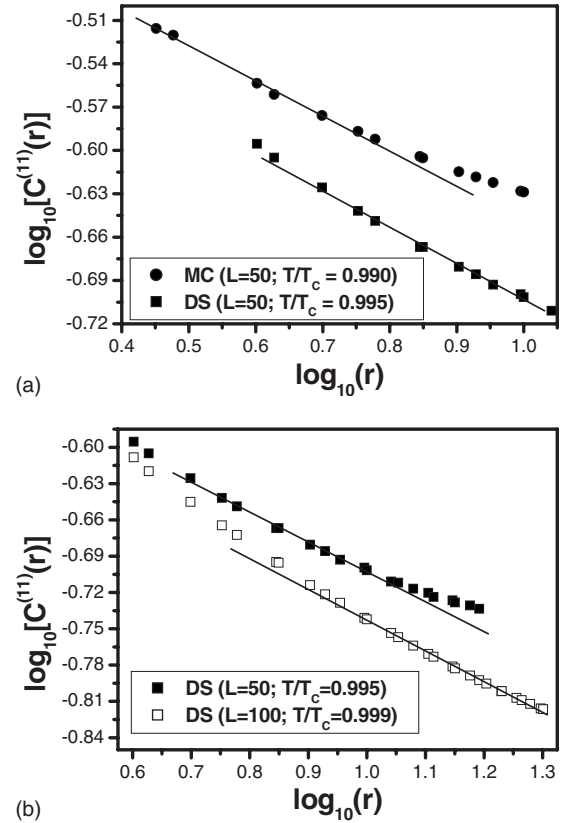


FIG. 3. Linear fits for the computation of the exponent  $\eta$ , associated with the correlation function  $C^{(1)}(r)$ . (a) The data obtained through standard MC simulations (black circles) and the present DS approach (black squares), for a square lattice of linear size  $L=50$ , are compared. One sees that the finite-size effects are reduced in the later procedure. (b) Data produced by the present DS approach for the sizes  $L=50$  (solid squares) and  $L=100$  (open squares).

case, the finite-size effects are weaker in the DS technique, leading essentially to an increase by a factor of 2 in the values of  $r$  that fit within the power-law behavior of Eq. (3.4). In Fig. 3(b) we exhibit the DS results for the two linear sizes analyzed: namely,  $L=50$  and  $L=100$ . One observes that this method produces data for the smaller size that are comparable to those of the larger size, showing the efficiency of the DS technique, in the sense that one may obtain accurate critical-exponent estimates from rather small lattice sizes; the two estimates for the exponent  $\eta$ , from Fig. 3(b), coincide, within the error bars. However, the range of validity of the power-law behavior, associated with the linear fit of Fig. 3(b), occurs for larger values of  $r$  in the case  $L=100$  (typically for  $7 < r < 20$ ), as expected. The reduction of finite-size effects was verified also in the magnetization curve, where one observes a smooth curve around criticality, followed by the well-known tail (characterized by  $m > 0$  for  $T > T_C$ ) within the MC method, whereas in the DS approach one finds a sharp curve around  $T_C$ , like the one shown in Fig. 2.

Although not expected to be relevant for the present model, the higher-order correlation functions and polarization parameter [defined in Eqs. (2.22) and (2.23), respectively] may be also computed within the present approach. Using time evolutions  $e_1, \dots, e_6$ , we calculated the correla-

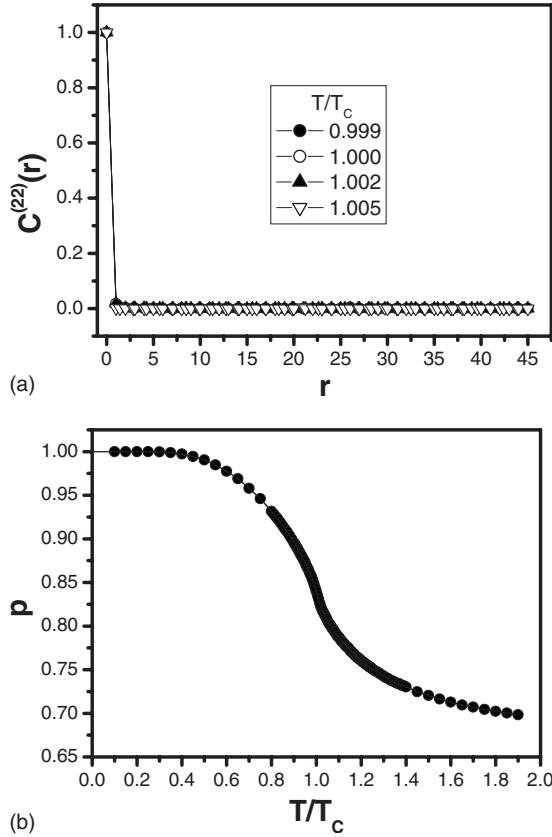


FIG. 4. (a) The correlation function  $C^{(22)}(r)$  versus  $r$ , for typical temperature ratios  $T/T_C$ , near criticality. (b) The polarization  $p$  versus  $T/T_C$ .

tion function  $C^{(22)}(r)$  and the polarization parameter for a linear size  $L=100$ , as exhibited in Fig. 4. For typical temperatures around  $T_C$ , the correlation function  $C^{(22)}(r)$  presents a trivial behavior for this model, i.e.,  $C^{(22)}(r)=0$ , for  $r>0$ , reflecting the absence of squared terms ( $L=D=0$ ) in the Hamiltonian considered in the present simulations. In what concerns the polarization, one gets a smooth behavior around  $T_C$ , suggesting that there is no phase transition associated with this parameter. One notices that the polarization approaches its expected asymptotic value for sufficiently

large temperatures, i.e.,  $p=2/3$ , since in this limit the spin variables should become equally distributed throughout its three possible states,  $S_i = \pm 1, 0$ . Although the quantities presented in Fig. 4 do not bring any additional physical information to the present model, they are relevant for other controversial spin-1 models in the literature, like the Blume-Capel ( $L=0; D \neq 0$ ) [24,25] and Blume-Emery-Griffithis ( $L \neq 0; D \neq 0$ ) [26] models, and may be computed also within the present approach.

#### IV. CONCLUSION

We have studied the nearest-neighbor-interaction spin-1 Ising model through the damage-spreading technique. Exact relations involving quantities computable through damage-spreading simulations and thermodynamic properties were derived for a general spin-1 model that covers several relevant and controversial particular cases of the literature. These relations hold for any ergodic dynamical procedure applied to translationally invariant systems. The implementation of the method was illustrated by performing damage-spreading simulations for the ferromagnetic spin-1 Ising model on a square lattice. Its effectiveness was verified through the computation of the two-spin correlation function and the magnetization, leading to precise estimates of the associated critical exponents, in spite of rather small lattice sizes. We have obtained the estimates

$$\beta = 0.1249 \pm 0.0003, \quad \eta = 0.2507 \pm 0.0025, \quad (4.1)$$

which fall in the same universality class of the spin-1/2 Ising model on two-dimensional lattices. Such results confirm the universality hypothesis for this model, which states that critical exponents should depend only on global properties of the model, like the dimension of the lattice and the symmetry of the order parameter. As far as we know, the two-spin correlation function has never been calculated numerically in the literature for the present model, and so it was estimated accurately herein within damage-spreading simulations. Combining the results obtained from both correlation function and magnetization, we have estimated the critical temperature,

$$\frac{k_B T_C}{J} = 1.692709 \pm 0.000847 \Rightarrow u_C = \exp[-J/(k_B T_C)] = 0.553901 \pm 0.000164, \quad (4.2)$$

which agrees, within the error bars, with the one estimated from an extensive low-temperature series expansion up to 79th order (Ref. [23]). These results reinforce the efficiency of the present method, which has also been established on other spin models [15,19,20], leading to a significant reduction of finite-size effects, when comparing with those produced by standard Monte Carlo simulations.

The present exact relations may be implemented also in damage-spreading numerical simulations on other translationally invariant nearest-neighbor interaction spin-1 models, opening the possibility of investigating more complicated and controversial models through this technique: (i) ferromagnetic models on hypercubic lattices ( $d > 2$ ), in order to test further the universality hypothesis; (ii) models character-

ized by squared-spin terms in the Hamiltonian, e.g., the Blume-Capel [24,25] and Blume-Emery-Griffithis [26] models, for which there are several controversies concerning their phase diagrams on  $d$ -dimensional lattices.

#### ACKNOWLEDGMENTS

The partial financial support from CNPq and Pronex/FAPERJ (Brazilian agencies) is acknowledged.

- 
- [1] H. Gould and J. Tobochnik, *An Introduction to Computer Simulation Methods*, 2nd ed. (Addison-Wesley, Reading, MA, 1996).
- [2] K. Binder and D. W. Heermann, *Monte Carlo Simulation in Statistical Physics* (Springer-Verlag, Berlin, 1988).
- [3] D. P. Landau and K. Binder, *A Guide to Monte Carlo Simulations in Statistical Physics* (Cambridge University Press, Cambridge, England, 2000).
- [4] H. E. Stanley, D. Stauffer, J. Kertész, and H. J. Herrmann, *Phys. Rev. Lett.* **59**, 2326 (1987).
- [5] B. Derrida and G. Weisbuch, *Europhys. Lett.* **4**, 657 (1987).
- [6] U. M. S. Costa, *J. Phys. A* **20**, L583 (1987).
- [7] G. Le Caër, *J. Phys. A* **22**, L647 (1989).
- [8] P. Grassberger, *J. Phys. A* **28**, L67 (1995).
- [9] A. M. Mariz, H. J. Herrmann, and L. de Arcangelis, *J. Stat. Phys.* **59**, 1043 (1990).
- [10] F. D. Nobre, A. M. Mariz, and E. S. Sousa, *Phys. Rev. Lett.* **69**, 13 (1992).
- [11] M. F. de A. Bibiano, F. G. Brady Moreira, and A. M. Mariz, *Phys. Rev. E* **55**, 1448 (1997).
- [12] L. da Silva, F. A. Tamarit, and A. C. N. Magalhães, *J. Phys. A* **30**, 2329 (1997).
- [13] E. M. de Sousa Luz, M. P. Almeida, U. M. S. Costa, and M. L. Lyra, *Physica A* **282**, 176 (2000).
- [14] J. A. Redinz, F. A. Tamarit, and A. C. N. Magalhães, *Physica A* **293**, 508 (2001).
- [15] A. Coniglio, L. de Arcangelis, H. J. Herrmann, and N. Jan, *Europhys. Lett.* **8**, 315 (1989).
- [16] A. M. Mariz, *J. Phys. A* **23**, 979 (1990).
- [17] A. M. Mariz, A. M. C. de Souza, and C. Tsallis, *J. Phys. A* **26**, L1007 (1993).
- [18] A. M. Mariz, E. S. de Sousa, and F. D. Nobre, *Physica A* **257**, 429 (1998).
- [19] A. S. Anjos, D. A. Moreira, A. M. Mariz, and F. D. Nobre, *Phys. Rev. E* **74**, 016703 (2006).
- [20] A. S. Anjos, D. A. Moreira, A. M. Mariz, F. D. Nobre, and F. A. da Costa, *Phys. Rev. E* **76**, 041137 (2007).
- [21] R. J. Baxter, *Exactly Solved Models in Statistical Mechanics* (Academic Press, London, 1982).
- [22] A. Lipowski and M. Suzuki, *J. Phys. Soc. Jpn.* **61**, 4356 (1992).
- [23] I. G. Enting, A. J. Guttmann, and I. Jensen, *J. Phys. A* **27**, 6987 (1994).
- [24] M. B. Blume, *Phys. Rev.* **141**, 517 (1966).
- [25] H. W. Capel, *Physica (Utrecht)* **32**, 966 (1966).
- [26] M. B. Blume, V. J. Emery, and R. B. Griffiths, *Phys. Rev. A* **4**, 1071 (1971).